Solid Freeform Fabrication 2017: Proceedings of the 28th Annual International Solid Freeform Fabrication Symposium – An Additive Manufacturing Conference
Reviewed Paper

SELECTIVE LASER MELTING OF NOVEL TITANIUM-TANTALUM ALLOY AS ORTHOPEDIC BIOMATERIAL

Florencia Edith Wiria [a,b], Swee Leong Sing [b,c], Wai Yee Yeong [a,c]

[a] Singapore Institute of Manufacturing Technology
73 Nanyang Drive, Singapore 637662
HW3-01-01, 65A Nanyang Drive, Singapore 637333
[b] SIMTech-NTU Joint Laboratory (3D Additive Manufacturing), Nanyang Technological University
HW1-01-05, 2A Nanyang Link, Singapore 637372
[c] Singapore Centre for 3D Printing, School of Mechanical & Aerospace Engineering, Nanyang Technological University

Abstract

Selective laser melting (SLM) is an additive manufacturing (AM) technique that is capable of fabricating complex functional three-dimensional (3D) metal parts directly from the complete melting and fusion of powders. As a powder bed fusion technology, SLM has the potential to expand its material library by forming alloys that were previously difficult to achieve by using metal powder mixtures that can be customized according to the application requirements.

Titanium-tantalum (TiTa) is a material that has potential uses in biomedical applications due to its high strength-to-modulus ratio. However, it is still not widely used because it is difficult to obtain. SLM is chosen as the method to form this alloy due to its versatility in processing metallic materials and good results obtained from commercially pure titanium (cpTi). Preliminary studies using cpTi lattice structures designed for biomedical applications were carried out. This research aims to develop TiTa as a material to be potentially used in biomedical field by investigating its processing window, resulting microstructure, and mechanical properties.

Introduction

Selective laser melting (SLM) is a powder bed additive manufacturing technique that uses laser power to fuse powder materials and form functional parts directly according to their computer aided design (CAD) data. Details of the SLM process are described in previous works [1-5]. Titanium alloys are excellent biomedical metal materials due to their excellent combination of corrosion resistance, mechanical properties, and biocompatibility [4]. Extensive research conducted on SLM of titanium alloys for biomedical applications includes Ti6Al4V [6-11] and Ti6Al7Nb [12-14]. However, there are safety concerns with these titanium alloy materials as they include aluminum, which may cause neurological issues in the human body after long term usage and/or cytotoxic vanadium [15-18]. There are motivations for developing new biomaterials that are free from these elements and have lower modulus to reduce the “stress shielding” effect.

Titanium-tantalum (TiTa) alloys are favorable as orthopedic biomaterials because of their low cost and high strength-to-density ratio [19]. However, TiTa alloys are still not widely applied mainly due to difficulties in alloying these two metals as they have great differences in

density and melting point [15]. Tantalum has a high density of 16.69 g/cm^3, while the density of titanium is 4.51 g/cm^3. This high difference in density could lead to inhomogeneity during alloying as the density difference may lead to segregation of alloying elements. The difference in melting point between these two elements can also lead to unneeded vaporization of titanium during the alloying process.

In this study, TiTa parts were processed using SLM. The feedstock is a mixture of tantalum and commercially pure titanium powders in equal weight percentages. The TiTa SLM processing window, resulting microstructure, and mechanical properties were investigated. Preliminary studies using cpTi lattice structures designed for biomedical applications were carried out and used to evaluate the suitability of TiTa as orthopedic biomaterial.

Materials and Methods

Both commercially pure titanium (cpTi) and tantalum powders are produced by gas atomization. The cpTi powder (Grade 2 ASTM B348, LPW Technology Ltd, United Kingdom) is spherical in shape and has particle size with average size of 43.5 μm. The tantalum powder (Singapore Demand Planner Ltd, Singapore) is irregular in shape and has average particle size of 44 μm. The two powders were mixed in weight ratio of 1:1 and then spun at a rate of 60 rpm for 12 hours using a tumbler mixer (Inversina 2L, Bioengineering AG). The mixed powder density was measured using gas displacement pycnometry system (AccuPyc II 1340, Micromeritics). Characterization of the powder mixture was done and detailed in previous work [20].

Fabrication of all the samples was carried out on a SLM 250HL machine (SLM Solutions Group AG, Germany). The SLM machine is equipped with a Gaussian beam fiber laser with maximum power of 400 W and a focal diameter of 80 μm. All processing occurred in an argon environment with less than 0.05 % oxygen to prevent oxidation and degradation of the material during the process. To minimize thermal stresses during the SLM process, sectorial (also known as island or chessboard) scanning was used.

Cubic samples of 10 mm × 10 mm × 10 mm were fabricated using the powder mixture in SLM to determine the processing window of TiTa. To optimize the processing parameters for fabrication of TiTa using SLM, a series of experiments were conducted by varying the hatch spacing and scanning speed while keeping the laser power and layer thickness constant at 360 W and 50 μm respectively. The processing parameters were optimized and chosen based on the relative density achieved for the sample and the formed macrostructure of the samples studied under light optical microscopy (LOM, Model SZX 7, Olympus). The samples' density was measured using a XS Analytical Balance (Model XS 204, Mettler Toledo), which is based on the Archimedes Principle. The details of the microstructural and mechanical characterization of TiTa have been reported previously [20].

The computer aided design (CAD) models of the cpTi lattice structures were designed and generated using Computer Aided System for Tissue Scaffolds (CASTS), which is the in-house developed library system consisting of 13 different polyhedral units that can be assembled into scaffold structures using programmed algorithms [21-23]. The polyhedral units chosen for this study were square pyramid, truncated cube, and truncated octahedron [21]. The dimensions of the repeating unit cell were 1 mm × 1 mm × 1 mm. The detailed illustrations of CASTS have been described by Chua *et al.* [24, 25]. The details of the mechanical characterization of these cpTi lattice structures have been reported previously [26].

Results and Discussion

The mixing procedure was effective in creating a homogenous powder blend of cpTi and tantalum powders, as shown in Figure 1.

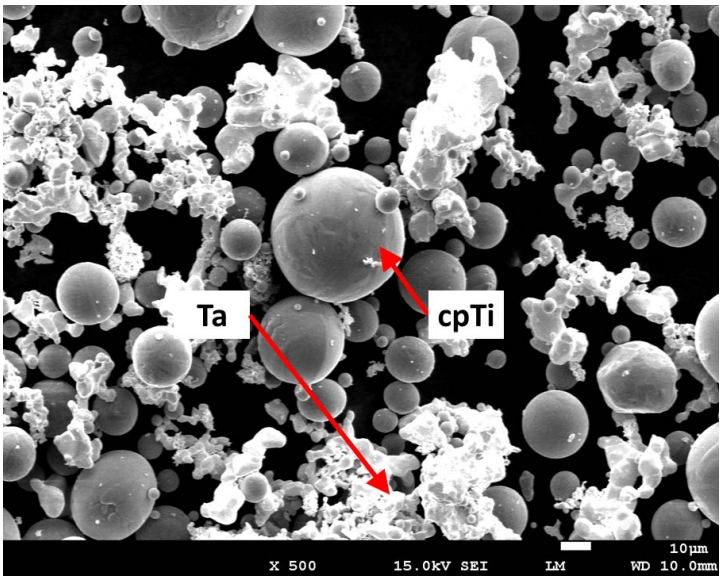

Figure 1: FESEM image of TiTa powder mixture

The titanium powder retained its spherical shape after the mixing, which is important for the powder mixture flowability. Tantalum powder has non-spherical shape, as its high melting point of 3020^{o} C restricts economical production of spherical powder. The overall flowability of the powder mixture is improved as spherical titanium particles easily roll and behave as a medium to push the tantalum powder during powder depositions.

The samples are studied under LOM to ascertain the macrostructure of the samples of various combination of processing parameters. The processing parameters used and the resulting surfaces in the x- and y-planes are shown in Figure 2.

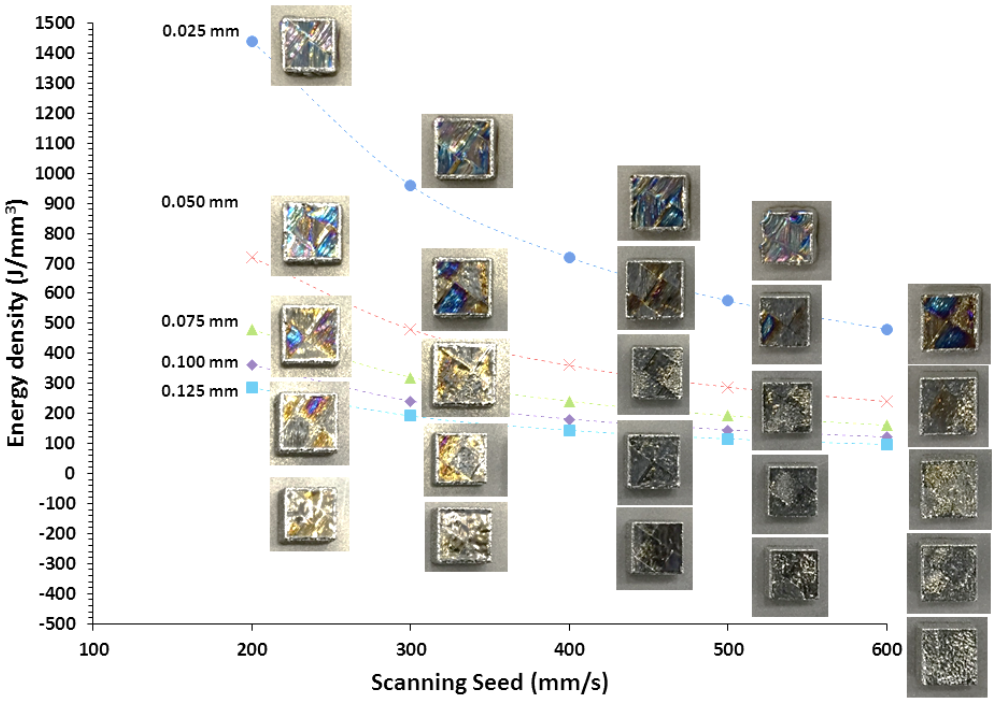

Figure 2: x- and y-plane surface morphology of density specimens with variation in energy density input

In a complex metallurgical process like SLM, optimizing the above mentioned inter-related parameters is crucial in producing high density and high quality parts. Unfavorable defects may occur in the parts due to localized irregularities such as balling, cracks, delamination, and residual stress. Balling is the droplet or fragmentation formation from the melt pool caused by capillary instability [27]. It occurs when the molten material does not wet the underlying substrate due to surface tension, which cause the liquid to form spheres. This results in a rough and bead-shaped surface, shown in Figure 3.

The beads obstruct homogenous layer deposition which decrease the density of the produced part. Furthermore, balling results in weak bonding between the melt tracks and causes the next powder layer to be deposited uniformly. This lead to a compounded effect and may form porosity and delamination caused by thermal stresses and weakened interlayer bonding [27]. Balling can be avoided by improving the stability of the melt pool. Cracks reduce mechanical properties of SLM parts significantly. Cracks in SLM parts could be classified into macroscopic and microscopic cracks. Macroscopic cracks are caused by stress induced crack propagation and low ductility of the material. Microscopic cracks are formed during rapid solidification due to liquid film interruption at grain boundaries, caused by tensile stress [27, 28]. Furthermore, unmelted or partially melted segments and porosity may be created due to improper powder deposition, leading to low and inhomogeneous powder bed density and solubility reduction of some elements in melt during solidification [29, 30]. These defects will lead to undesirable effects on the relative density of the SLM parts. The relative density of the specimens with variation of energy density input is shown in Figure 3.

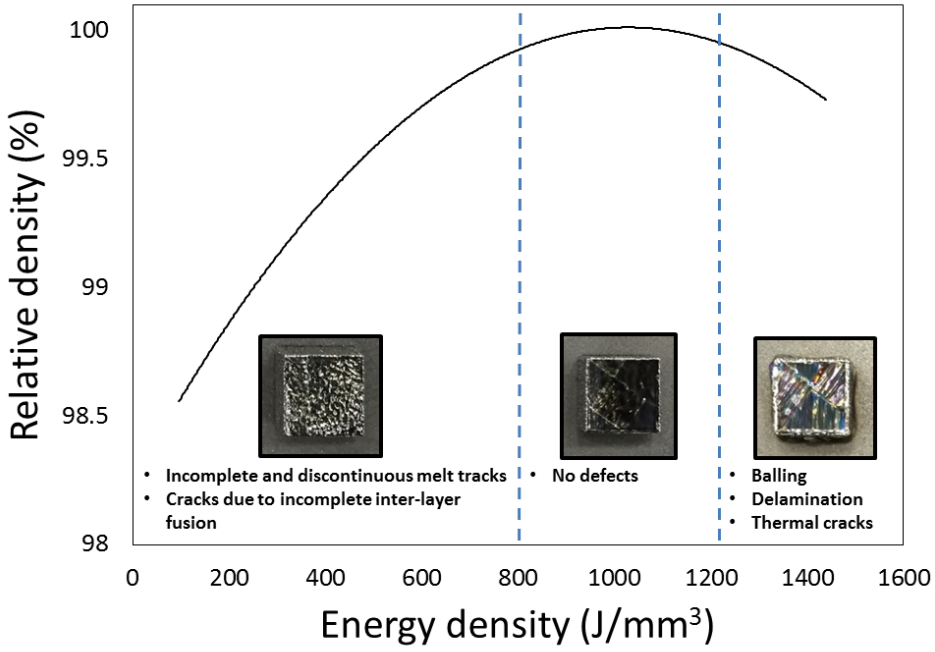

Figure 3: Relative density of TiTa cubic parts with variation in energy density input

Good TiTa parts were obtained by optimizing the SLM processing parameters. Figure 4 shows microstructures of the SLM parts in xy- and yz-plane. Based on the characterization results, it is confirmed that the SLM TiTa consists only of β phase, which was caused by a tantalum stabilizing effect of the phase after rapid solidification. Details of the forming mechanisms of SLM TiTa have also been described previously [20].

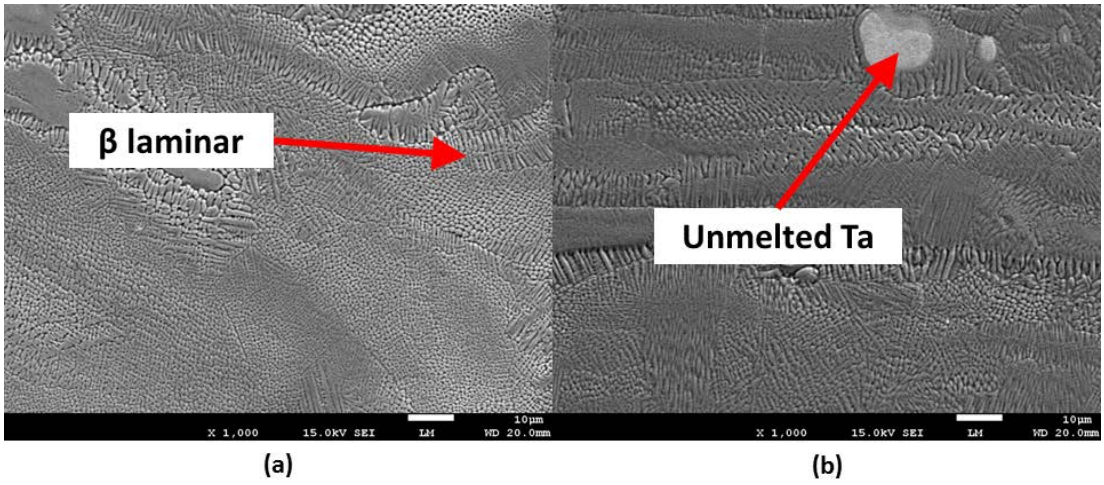

Figure 4: Micrograph of TiTa samples in (a) xy- and (b) yz-plane

The SLM produced samples consist of TiTa solid solution matrix with small amount of unmelted tantalum particles. The energy applied during SLM is sufficient to melt the titanium powder fully but some of the larger tantalum particles only melted partially due to the higher melting point of tantalum. Furthermore, the relatively large two phase (liquid + solid) field in the binary titanium-tantalum phase diagram also shows the difficulty in melting the two materials together. This resulted in the tantalum particles in TiTa matrix microstructure.

The SLM TiTa has modulus of 75.77 ± 4.04 GPa, ultimate tensile strength of 924.64 ± 9.06 MPa, and yield strength of 882.77 ± 19.60 MPa. It was characterized using test standard from ASTM E8. The SLM TiTa modulus is lower compared to SLM cpTi and SLM Ti6Al4V fabricated using similar parameters [20]. Despite the lower modulus, SLM TiTa still has modulus higher than the wide range of human bone modulus, for example from 6.9 to 25.0 GPa [31]. Hence, there is a need to lower the modulus of TiTa by creating porous lattice structure designs for the use in orthopaedic applications.

As a preliminary study, cpTi is used to fabricate the lattice structures, and the characterization of these structures has been reported previously [26]. Samples of the lattice structures fabricated are shown in Figure 5.

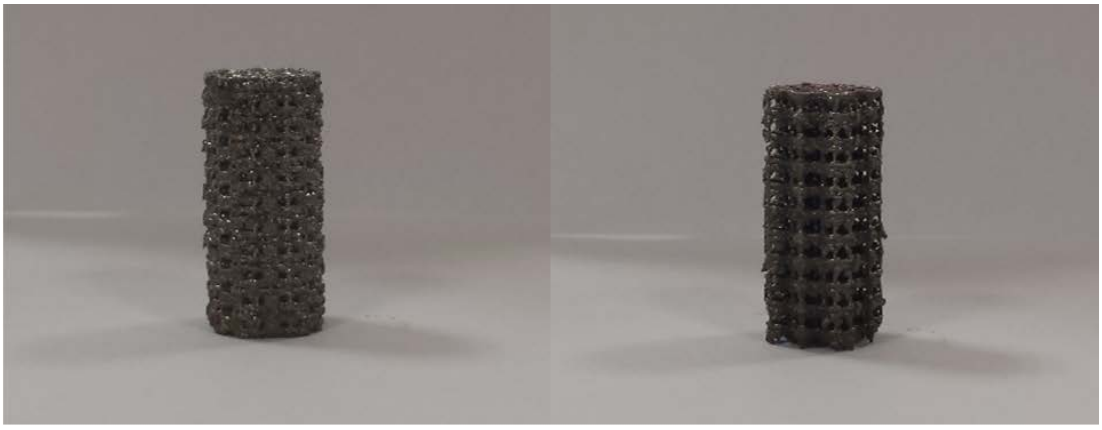

Figure 5: Samples of cpTi lattice structures (a) square pyramid (b) truncated cube & octahedron unit cells

Using Gibson–Ashby model [32], the modulus of the lattice structures can be estimated as shown in Table 2, where E and ρ are the apparent Young's modulus and density of the lattice structures, E_0 and ρ_0 are the modulus, density of fully dense material, respectively.

Table 1: Gibson–Ashby model for lattice structures

Unit cells	
Square pyramid	$\frac{E}{E_0} = 0.377\left(\frac{\rho}{\rho_0}\right)^2$
Truncated cube & octahedron	$\frac{E}{E_0} = 0.206\left(\frac{\rho}{\rho_0}\right)^2$

To obtain modulus of human bone using TiTa lattice structures, the porosity of the lattice structures need to be lower than 50.9 % and 33.5 % for the square pyramid, truncated cube, and truncated octahedron unit cells, respectively. These porosity levels can be achieved by SLM by changing the unit cells dimensions, such as strut size.

Conclusions

This study investigated the feasibility of alloying metals using metal powder mixture as feedstock for SLM. From the results, TiTa parts were manufactured via SLM successfully, showing SLM as a feasible process in alloying materials. To ascertain TiTa as biomaterial for orthopedic applications, preliminary studies using cpTi lattice structures designed for biomedical applications were carried out.

As the modulus of bulk SLM TiTa is still higher than modulus of human bones, results from cpTi lattice structures were used to evaluate the suitability of using TiTa lattice structures in biomedical applications. The results shown are promising as TiTa lattice structures need to have porosity of at least 33.5 % to achieve human bone modulus, which is achievable by design and fabrication using SLM.

References

[1] S.L. Sing, W.Y. Yeong, C.K. Chua, F.E. Wiria, Z.H. Liu, D.Q. Zhang, B.Y. Tay, Classical lamination theory applied on parts produced by selective laser melting, High Value Manufacturing: Advanced Research in Virtual and Rapid Prototyping, (2013) 77-82.

[2] C.Y. Yap, C.K. Chua, Z.L. Dong, Z.H. Liu, D.Q. Zhang, L.E. Loh, S.L. Sing, Review of selective laser melting: Materials and applications, Applied Physics Reviews, 2 (2015) 041101.

[3] L.E. Loh, C.K. Chua, W.Y. Yeong, J. Song, M. Mapar, S.L. Sing, Z.H. Liu, D.Q. Zhang, Numerical investigation and an effective modelling on the Selective Laser Melting (SLM) process with aluminium alloy 6061, International Journal of Heat and Mass Transfer, 80 (2015) 288-300.

[4] S.L. Sing, J. An, W.Y. Yeong, F.E. Wiria, Laser and electron-beam powder-bed additive manufacturing of metallic implants: A review on processes, materials and designs, Journal of Orthopaedic Research, 34 (2016) 369-385.

[5] Z.H. Liu, D.Q. Zhang, S.L. Sing, C.K. Chua, L.E. Loh, Interfacial characterization of SLM parts in multi-material processing: Metallurgical diffusion between 316L stainless steel and C18400 copper alloy, Materials Characterization, 94 (2014) 116-125.

[6] E. Sallica-Leva, A.L. Jardini, J.B. Fogagnolo, Microstructure and mechanical behavior of porous Ti-6Al-4V parts obtained by selective laser melting, Journal of the Mechanical Behavior of Biomedical Materials, 26 (2013) 98-108.

[7] J.F. Sun, Y.Q. Yang, D. Wang, Mechanical properties of a Ti6Al4V porous structure produced by selective laser melting, Materials & Design, 49 (2013) 545-552.

[8] L. Facchini, E. Magalini, P. Robotti, A. Molinari, S. Höges, K. Wissenbach, Ductility of a Ti-6Al-4V alloy produced by selective laser melting of prealloyed powders, Rapid Prototyping Journal, 16 (2010) 450-459.

[9] L.E. Murr, S.A. Quinones, S.M. Gaytan, M.I. Lopez, A. Rodela, E.Y. Martinez, D.H. Hernandez, E. Martinez, F. Medina, R.B. Wicker, Microstructure and mechanical behavior of Ti-6Al-4V produced by rapid-layer manufacturing, for biomedical applications, Journal of the Mechanical Behavior of Biomedical Materials, 2 (2009) 20-32.

[10] B. Vrancken, L. Thijs, J.-P. Kruth, J. Van Humbeeck, Heat treatment of Ti6Al4V produced by Selective Laser Melting: Microstructure and mechanical properties, Journal of Alloys and Compounds, 541 (2012) 177-185.
[11] L. Thijs, F. Verhaeghe, T. Craeghs, J. Van Humbeeck, J.-P. Kruth, A study of the microstructural evolution during selective laser melting of Ti-6Al-4V, Acta Materialia, 58 (2010) 3303-3312.
[12] E. Chlebus, B. Kuznicka, T. Kurzynowski, B. Dybala, Microstructure and mechanical behaviour of Ti-6Al-7Nb alloy produced by selective laser melting, Materials Characterization, 62 (2011) 488-495.
[13] H. Rotaru, G. Armencea, D. Spîrchez, C. Berce, T. Marcu, D. Leordean, S.G. Kim, S.W. Lee, C. Dinu, G. Băciuţ, M. Băciuţ, In vivo behavior of surface modified Ti6Al7Nb alloys used in selective laser melting for custom-made implants. A preliminary study, Romanian Journal of Morphology and Embryology, 54 (2013) 791-796.
[14] P. Szymczyk, A. Junka, G. Ziólkowski, D. Smutnicka, M. Bartoszewicz, E. Chlebus, The ability of S.aureus to form biofilm on the TI-6Al-7Nb scaffolds produced by Selective Laser Melting and subjected to the different types of surface modifications, Acta of Bioengineering and Biomechanics, 15 (2013) 69-76.
[15] A. Morita, H. Fukui, H. Tadano, S. Hayashi, J. Hasegawa, M. Niinomi, Alloying titanium and tantalum by cold crucible levitation melting (CCLM) furnace, Materials Science and Engineering: A, 280 (2000) 208-213.
[16] P. Laheurte, F. Prima, A. Eberhardt, T. Gloriant, M. Wary, E. Patoor, Mechanical properties of low modulus β titanium alloys designed from the electronic approach, Journal of the Mechanical Behavior of Biomedical Materials, 3 (2010) 565-573.
[17] J. Máleka, F. Hnilicaa, J. Veselýa, B. Smolac, S. Bartákovád, J. Vaněkd, Microstructure and mechanical properties of Ti-35Nb-6Ta alloy after thermomechanical treatment, Materials Characterization, 66 (2012) 75-82.
[18] R. Banerjee, S. Nag, J. Stechschulte, H.L. Fraser, Strengthening mechanisms in Ti-Nb-Zr-Ta and Ti-Mo-Zr-Fe orthopaedic alloys, Biomaterials, 25 (2004) 3413-3419.
[19] K.A. de Souza, A. Robin, Preparation and characterization of Ti-Ta alloys for application in corrosive media, Materials Letters, 57 (2003) 3010-3016.
[20] S.L. Sing, W.Y. Yeong, F.E. Wiria, Selective laser melting of titanium alloy with 50 wt% tantalum: Microstructure and mechanical properties, Journal of Alloys and Compounds, 660 (2016) 461-470.
[21] N. Sudarmadji, J.Y. Tan, K.F. Leong, C.K. Chua, Y.T. Loh, Investigation of the mechanical properties and porosity relationships in selective laser-sintered polyhedral for functionally graded scaffolds, Acta biomaterialia, 7 (2011) 530-537.
[22] M.W. Naing, C.K. Chua, K.F. Leong, Y. Wang, Fabrication of customised scaffolds using computer-aided design and rapid prototyping techniques, Rapid Prototyping Journal, 11 (2005) 249-259.
[23] W.Y. Yeong, N. Sudarmadji, H.Y. Yu, C.K. Chua, K.F. Leong, S.S. Venkatraman, Y.C. Boey, L.P. Tan, Porous polycaprolactone scaffold for cardiac tissue engineering fabricated by selective laser sintering, Acta biomaterialia, 6 (2010) 2028-2034.
[24] C.K. Chua, K.F. Leong, C.M. Cheah, S.W. Chua, Development of a tissue engineering scaffold structure library for rapid prototyping. Part 1: Investigation and classification, International Journal of Advanced Manufacturing Technology, 21 (2003) 291-301.
[25] C.K. Chua, K.F. Leong, C.M. Cheah, S.W. Chua, Development of a tissue engineering scaffold structure library for rapid prototyping. Part 2: Parametric library and assembly program, International Journal of Advanced Manufacturing Technology, 21 (2003) 302-312.

[26] S.L. Sing, W.Y. Yeong, F.E. Wiria, B.Y. Tay, Characterization of Titanium Lattice Structures Fabricated by Selective Laser Melting Using an Adapted Compressive Test Method, Experimental Mechanics, (2016).
[27] D.D. Gu, W. Meiners, K. Wissenbach, R. Poprawe, Laser additive manufacturing of metallic components: materials, processes and mechanisms, International Materials Reviews, 57 (2012) 133-164.
[28] M. Zhong, H. Sun, W. Liu, X. Zhu, J. He, Boundary liquation and interface cracking characterization in laser deposition of Inconel 738 on directionally solidified Ni-based superalloy, Scripta Materialia, 53 (2005) 159-164.
[29] J.P. Kruth, G. Levy, F. Klocke, T.H.C. Childs, Consolidation phenomena in laser and powder-bed based layered manufacturing, CIRP Annals - Manufacturing Technology, 56 (2007) 730-759.
[30] K.G. Prashanth, S. Scudino, H.J. Klauss, K.B. Surreddi, L. Löber, Z. Wang, A.K. Chaubey, U. Kühn, J. Eckert, Microstructure and mechanical properties of Al-12Si produced by selective laser melting: Effect of heat treatment, Material Science and Engineering: A, 590 (2014) 153-160.
[31] P.K.Z. Zysset, X.E. Guo, C.E. Hoffler, K.E. Moore, S.A. Goldstein, Elastic modulus and hardness of cortical and trabecular bone lamellae measured by nanoindentation in the human femur, Journal of Biomechanics, 32 (1999) 1005-1012.
[32] L.J. Gibson, M.F. Ashby, Cellular solids: structures and properties, 2nd edition ed., Cambridge University Press, New York, 1997.